

<http://ansinet.com/itj>

ITJ

ISSN 1812-5638

INFORMATION TECHNOLOGY JOURNAL

ANSI*net*

Asian Network for Scientific Information
308 Lasani Town, Sargodha Road, Faisalabad - Pakistan

Design of an Interval Type-2 Fuzzy Immune Controller

Chan-Hong Chao, Ming-Ying Hsiao, Shun-Hung Tsai and Tzoo-Hseng S. Li
Department of Electrical Engineering, National Cheng Kung University,
Tainan 701, Taiwan, Republic of China

Abstract: This study presents a novel Interval Type-2 Fuzzy Immune Control (IT2FIC) for linear and nonlinear discrete systems. The controller is designed by integration of the Interval Type-2 Fuzzy Logic Control (IT2FLC) and immune feedback control law. The type-2 fuzzy logic system is adopted to approximate the undetermined nonlinear function of the immune system. In order to reduce the computational loads of the type-reduction process, a new algorithm is proposed for type-reduction with a geometric analysis, which is utilized to derive a formula for computational geometry. Finally, the computer simulation results demonstrate that the proposed IT2FIC can obtain the best tracking performance among the Type-1 Fuzzy Logic Control (T1FLC), the IT2FIC and the Type-1 Fuzzy Immune Control (T1FIC).

Key words: Fuzzy immune control, immune feedback control law, immune system, nonlinear discrete system, type-2 fuzzy logic control

INTRODUCTION

For decades, growth in the understanding of several computational intelligence approaches, such as artificial neural networks (Culibrk *et al.*, 2007), fuzzy systems (Linfeng *et al.*, 2009), evolutionary algorithms (Zhihuan *et al.*, 2010) and artificial immune systems (Yu *et al.*, 2007), has led to propose a soft computing paradigm. The biological immune system has properties that have very strong robustness and high self-adaptability even in the face of uncertain situations and unexpected disturbances. Thus, it is hoped that this immune system will provide new paradigms appropriate for dynamic systems under unknown environments (Luh and Liu, 2008).

Basically, bone marrow is a type of soft tissue which can be found in the cavity of elongated bones. During the differentiation of a blood cell into a B-cell, bone marrow can produce and exhibit an antibody molecule on its surface. An antibody molecule has two main functions, one is to bind with an antigen and the other is to perform an effector function. The primary function occurs when the immune system first encounters an antigen. As it learns about the antigen, it prepares the body against further invasion by that antigen, thus creating memory in the immune system. The secondary function occurs when the same antigen is encountered. This response exhibits a quicker and more abundant production of antibodies

(Takahashi and Yamada, 1998; Yu *et al.*, 2007). When a naive B-cell encounters an antigen molecule through its receptor, the cell is activated and begins dividing rapidly; the cells from these B cells differentiate into memory B cells and effector B cells or plasma cells.

Fuzzy logic controls have been successfully applied to a wide variety of domain areas, such as bilinear systems (Li *et al.*, 2008), car-like mobile robots, robot manipulators and visual servoing (Linfeng *et al.*, 2009). The concept of type-2 fuzzy sets (T2FSs) was first introduced by Zadeh (1975) as an extension of the concept of well known ordinary fuzzy sets, type-1 fuzzy sets. Typically, T2FSs have the characteristics of grades of membership fuzzy themselves. A type-2 fuzzy set is characterized by a fuzzy membership function, i.e., the membership grade for each element is also a fuzzy set in $[0,1]$ (Hsiao *et al.*, 2008; Kamik *et al.*, 1999), unlike a type-1 fuzzy set, where the membership grade is a crisp number in $[0,1]$. The membership functions of type-2 fuzzy sets are three-dimensional and include a Footprint of Uncertainty (FOU), which is the new third dimension of type-2 fuzzy sets. The footprint of uncertainty provides an additional degree of freedom to make it possible to directly model and handle uncertainties. The type-2 fuzzy sets are useful especially when it is difficult to determine the exact and precise membership functions.

The type-2 fuzzy logic system was coined by Karnik and Mendel (1998) and it can be used under

uncertain circumstances when the membership grades can not be determined exactly. For systems with uncertainties and disturbances, the type-2 fuzzy logic system can outperform a conventional fuzzy logic system (Hsiao *et al.*, 2008; Wu and Mendel, 2007).

In this study, we propose a novel interval type-2 fuzzy immune control for a class of discrete nonlinear systems, which combine type-2 fuzzy logic and immune systems. This controller can provide more robustness than that of the conventional FLC and also handle uncertainties and disturbances.

IMMUNE FEEDBACK CONTROL DESIGN

The helper T-cell T_H in the immune system acts as a stimulant to the B cell, while the inhibitory T-cell acts as an inhibitor to the B cell. Suppose that the k -th generation of the antigen is $\epsilon(k)$, the output of the stimulated helper T-cell from the antigen is $T_H(k)$ and the inhibition of the B cell from the inhibitory T-cell restrained is $T_S(k)$, then, the total stimulation received by the B cell can be expressed as (Takahashi and Yamada, 1998; Kan *et al.*, 2008):

$$S_B(k) = T_H(k) - T_S(k) \quad (1)$$

$$T_H(k) = K_H(k)\epsilon(k) \quad (2)$$

$$T_S(k) = K_S f(S_B(k), \Delta S_B(k))\epsilon(k) \quad (3)$$

where, $f(S_B(k), \Delta S_B(k))$ is a nonlinear function that presents the relation between the output of the T_S cell and the antigen, i.e., the magnitude of the inhibition capability of the cell.

If we consider that the total stimulation that the B cells receive is the control input $u(k)$ and the amount of antigen is $\epsilon(k)$, which is equal to $|e(k)| \cdot \text{sign}(e(k) + \lambda(e(k) - e(k-1))/T)$, where $e(k) = r(k) - y(k)$, then the feedback control law can be obtained as follows:

$$\begin{aligned} u(k) &= K_H \cdot \text{sign}(e(k) + \lambda(e(k) - e(k-1))/T) - K_S f(u(k-1), \Delta u(k-1)) \\ &\quad \cdot |e(k)| \cdot \text{sign}(e(k) + \lambda(e(k) - e(k-1))/T) \\ &= K_H \left\{ 1 - \frac{K_H}{K_S} f(u(k-1), \Delta u(k-1)) \right\} \cdot |e(k)| \cdot \\ &\quad \text{sign}(e(k) + \lambda(e(k) - e(k-1))/T) \\ &= K_H \left\{ 1 - \eta f(u(k-1), \Delta u(k-1)) \right\} \cdot |e(k)| \cdot \\ &\quad \text{sign}(e(k) + \lambda(e(k) - e(k-1))/T) \end{aligned} \quad (4)$$

where $\Delta u(k-1) = u(k-1) - u(k-2)$, K_H , K_S and λ are scaling factors, K_H is the reactive rate and $\eta = K_H/K_S$ is utilized to control the stabilization effect. Now, the nonlinear function $f(u(k-1), \Delta u(k-1))$ will be approximated by using a type-2 fuzzy logic system.

The selection of $f(u(k-1), \Delta u(k-1))$ in Eq. 4 may affect the performance of the controlled system and the fuzzy system is a universal approximator for a nonlinear system (Dianyou *et al.*, 2007; Wang and Mendel, 1992). Here, we adopt the interval type-2 fuzzy system to approximate the nonlinear terms in the immune system. The control input $u(k-1)$ and its variation $\Delta u(k-1)$ of the immune system are also the control inputs of the type-2 fuzzy system, which is shown in Fig. 1. It is not necessary to know the precise model of immune system when designing the type-2 fuzzy controller.

INTERVAL TYPE-2 FUZZY IMMUNE CONTROL DESIGN

The design procedures for an interval type-2 fuzzy logic controller will be introduced here. The architecture of the type-2 fuzzy logic system is very similar to that of the conventional fuzzy logic system (type-1 fuzzy logical system), but its antecedent and/or consequent sets are now at least one of these sets and are clarified as type-2 fuzzy sets. The major difference is the output processor, which includes the type-reducer and the defuzzifier: while the former outputs type-1 fuzzy sets, the latter outputs a crisp number. The T2FLCs can be used under uncertain

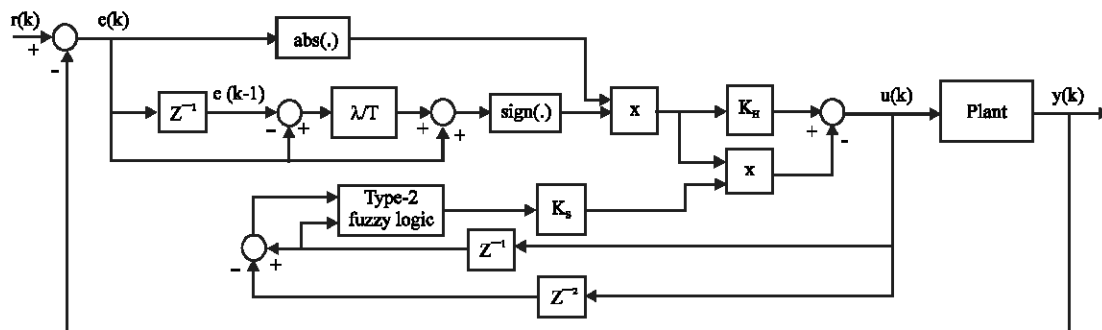


Fig. 1: The block diagram of the internal type-2 fuzzy immune control system

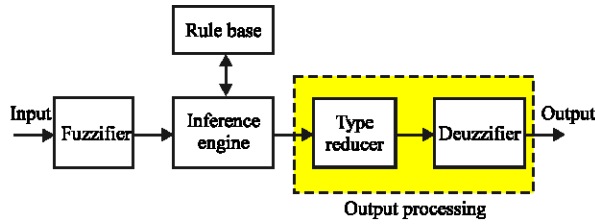


Fig. 2: The architecture of the type-2 fuzzy logic system

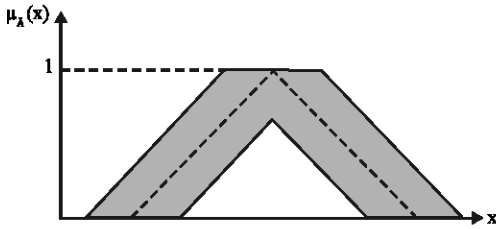


Fig. 3: The triangular shape interval type-2 fuzzy set

circumstances when the membership grades can not be determined exactly. Normally, T2FLCs have characteristics of intensive computation due to the heavy computational load at the step of the type reducing process, which can be simplified a lot if their secondary membership functions are chosen as the interval sets. Figure 2 shows the architecture of the type-2 fuzzy logic system, which contains a fuzzifier, rule table, inference engine, type-reducer and defuzzifier.

Fuzzifier: The fuzzifier nonlinearly maps the input crisp values into interval type-2 fuzzy sets. It is obvious that the type-2 fuzzy set is in a region constructed by a principal type-1 fuzzy set as shown in Fig. 3. The dotted line in Fig. 3 represents the primary membership function, while the shaded region is the FOU. The type-2 fuzzy sets can also be represented by a collection of many embedded type-1 fuzzy sets.

For using a fuzzy system to approximate the nonlinear function $f(u(k-1), \Delta u(k-1))$, the input variables $u(k-1)$, and $\Delta u(k-1)$ are mapped into three partitions as N (Negative), Z (Zero) and P (Positive), which is shown in Fig. 4. For the THEN-part, a singleton with uncertain width membership function is selected and is also partitioned into N (Negative), Z (Zero) and P (Positive), as shown in Fig. 5.

Rule tables: The rules for a type-2 fuzzy logic system still remain the same as those for type-1 fuzzy logic system T1FLC, but at least one of their antecedents and the consequents will be represented by interval type-2 fuzzy sets.

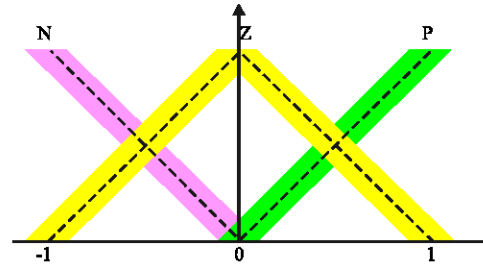


Fig. 4: The membership functions of IF-part

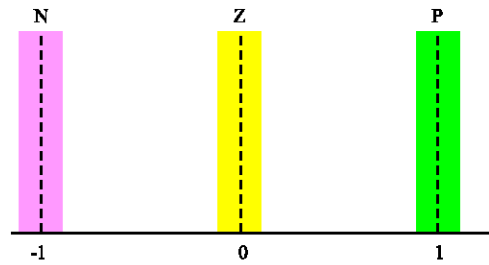


Fig. 5: The membership functions of THEN-part

Table 1: Rule table for T1FIC and IT2FIC

$f(\bullet, \bullet)$	$\Delta u(k-1)$		
	N	Z	P
$u(k-1)$			
N	P	P	Z
Z	P	Z	N
P	Z	N	N

Based on the biological phenomena, the smaller the T_s cell that receives the stimulus, the greater the suppression is and vice versa. We construct a 9-rule fuzzy table shown in Table 1.

Consider an IT2FLC with two inputs $u(k-1)$ and $\Delta u(k-1)$ and a single output $f(u(k-1), \Delta u(k-1))$, then the n -th rule for IT2FLC can be written as:

$$\begin{aligned} \text{If} & \quad (u(k-1) \text{ is } A_n \text{ and } \Delta u(k-1) \text{ is } B_n) \\ \text{Then} & \quad f(u(k-1), \Delta u(k-1)) \text{ is } D_n \text{ for } n = 1, 2, \dots, N \end{aligned} \quad (5)$$

Inference engine: The inference engine nonlinearly maps all the fired rules from input T2FS to output T2FS. Multiple antecedents in each rule are connected by using the Meet operation. The membership grades in the input sets are combined with those in the output sets by using the extended sup-star composition and multiple rules are combined by using the join operation.

It is necessary to find out the upper and lower bounds for each firing interval fuzzy set before the defuzzification method. As the membership grade can be obtained by using the Max-Min method in a type-1 fuzzy

logic system, similarly, we adopt this Max-Min scheme to find the upper and lower bounds of the fired resulting interval sets. The detailed procedures are described as follows.

The upper bound of the interval type-2 fuzzy sets α_n^A and α_n^B can be expressed as:

$$\bar{\alpha}_n^A = \max \left\{ \min_{i \in M} \left[\bar{u}^i, \bar{A}_n^i \right] \right\} \quad (6a)$$

$$\bar{\alpha}_n^B = \max \left\{ \min_{i \in M} \left[\bar{\Delta u}^i, \bar{B}_n^i \right] \right\} \quad (6b)$$

Its associated upper bound of weighting value for the n-th fuzzy rule can be obtained by:

$$\bar{w}_n = \min \left(\bar{\alpha}_n^A, \bar{\alpha}_n^B \right) \quad (7)$$

The upper bound of output for the n-th fuzzy rule can be obtained by:

$$\bar{f}_n^i = \min_{i \in M} \left\{ \bar{w}_n, \bar{D}_n^i \right\} \quad (8)$$

So, the upper bound of the resulting interval set can be expressed as:

$$\bar{f}^i = \max \left\{ \bar{f}_1^i, \dots, \bar{f}_N^i \right\} \quad (9)$$

Similarly, the lower bound can be expressed as:

$$\underline{\alpha}_n^A = \max \left\{ \min_{i \in M} \left[\underline{u}^i, \underline{A}_n^i \right] \right\} \quad (10a)$$

$$\underline{\alpha}_n^B = \max \left\{ \min_{i \in M} \left[\underline{\Delta u}^i, \underline{B}_n^i \right] \right\} \quad (10b)$$

Its associated lower bound of weighting value for the n-th fuzzy rule can be obtained by:

$$\underline{w}_n = \min \left(\underline{\alpha}_n^A, \underline{\alpha}_n^B \right) \quad (11)$$

The lower bound of output for the n-th fuzzy rule can be obtained by:

$$\underline{f}_n^i = \min_{i \in M} \left\{ \underline{w}_n, \underline{D}_n^i \right\} \quad (12)$$

So, the lower bound of the resulting interval set can be expressed as:

$$\underline{f}^i = \max \left\{ \underline{f}_1^i, \dots, \underline{f}_N^i \right\} \quad (13)$$

The summation of the inference resulting interval set from each fired rule can be expressed with the upper and lower bounds as:

$$F = \left[\underline{f}^i, \bar{f}^i \right] \quad (14)$$

The inference process can be illustrated graphically as in Fig. 6.

Type-reducer: The output processor includes a type-reducer and defuzzifier. The type-reduction method is an extension of type-1 defuzzification obtained by applying the Extension Principle to a specific defuzzification method (Visconti and Tahayori, 2008). The type-reduced set using the Center of Sets (COS) type-reduction can be expressed as:

$$C_{cos}(U) = [C_{L_{min}}, C_{R_{max}}] = \frac{\int_{c \in [c_L^i, c_k^i]} \dots \int_{c \in [c_k^i, c_k^i]} \dots \int_{c \in [c_k^i, c_k^i]} \dots \int_{c \in [c_k^i, c_k^i]} 1 \cdot \frac{\sum_{i=1}^M f^i c^i}{\sum_{i=1}^M f^i} \quad (15)$$

where, $U = [u(k-1) \quad \Delta u(k-1)]^T$, is the input of the IT2FLC. Determination of the interval set $[C_{L_{min}}, C_{R_{max}}]$ is described follows.

The left-most minimum $C_{L_{min}}$: As the left-most minimum $C_{L_{min}}$ of the type-reduced set is not just simply to calculate the center of gravity of the lower bound of the fired membership grades, we need to determine point to rearrange all the fired interval sets to find the center of gravity, i.e., to determine the weighting of each membership function.

From the weighting methodology, we take the left-hand side of the test point p as \bar{f}_i and the right-hand side of the test point P as \underline{f}_i , respectively, as shown in Fig. 7a. As point P intersects the first singleton output set, C_L can be obtained by:

$$C_L = \frac{\Delta x \left(\sum_{i=1}^N \bar{f}_i y_i \right) + (\bar{f}_k - \underline{f}_k) \left[P - \left(y_k - \frac{\Delta x}{2} \right) \right] \cdot \left[\left(\frac{y_k - \frac{\Delta x}{2} + P}{2} \right) \right]}{\Delta x \left(\sum_{i=1}^N \bar{f}_i \right) + (\bar{f}_k - \underline{f}_k) \left[P - \left(y_k - \frac{\Delta x}{2} \right) \right]} \quad (16)$$

where, Δx is the span of uncertainty and y_i is the i-th centroid of the consequent output set. while point P intersects the second or beyond the second singleton output set, shown in Fig. 7b, C_L can be calculated by:

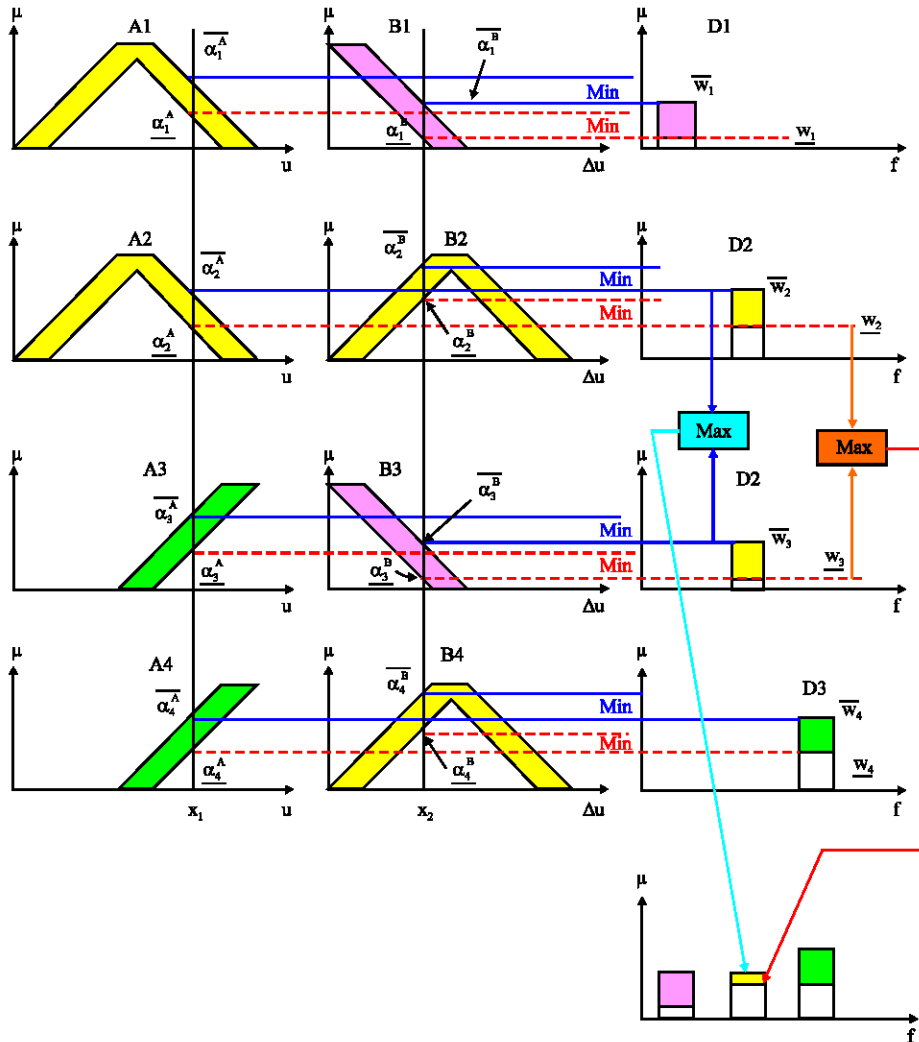


Fig. 6: Graphic illustration of the interval type-2 fuzzy implication

$$C_L = \frac{\Delta x \left(\sum_{i=1}^N f_i y_i \right) + \Delta x \cdot \sum_{j=1}^{k-1} (\bar{f}_j - \underline{f}_j) \cdot y_j + (\bar{f}_k - \underline{f}_k) \left[P - \left(y_k - \frac{\Delta x}{2} \right) \right] \cdot \left[\left(\frac{y_k - \Delta x}{2} + \frac{P}{4} \right) \right]}{\Delta x \left(\sum_{i=1}^N \underline{f}_i \right) + \Delta x \cdot \sum_{j=1}^{k-1} (\bar{f}_j - \underline{f}_j) + (\bar{f}_k - \underline{f}_k) \left[P - \left(y_k - \frac{\Delta x}{2} \right) \right]} \quad (17)$$

where, N is the number of triggered membership functions. The parameter k can be obtained by the following If-Then rule.

$$\text{If } P > \left(y_i - \frac{\Delta x}{2} \right) \text{ then } k = i \quad (18)$$

The iteration procedures to obtain the minimum value of $C_{L_{\max}}$ are described as follows:

- Step 1:** Set $n = n+1$
- Step 2:** Compute $C_L(n)$
- Step 3:** If $(1 < n)$ and $(n \leq M)$, then $C_L(n) = \min[C_L(n-1), C_L(n)]$
- Step 4:** If $n = M$ then stop
- Step 5:** Return to step 1

The right-most maximum $C_{R_{\max}}$: Calculation of $C_{R_{\max}}$ is very similar to that of $C_{L_{\max}}$. Based on the schemes for evaluating $C_{L_{\max}}$ mentioned in the previous subsection, we take the left-hand side of the test point P as \underline{f}_i and the right-hand side of the test point P as \bar{f}_i , respectively, as shown in Fig. 8. As point P intersects the first output set, shown in Fig. 8a, C_R can be obtained by using the center of gravity approach,

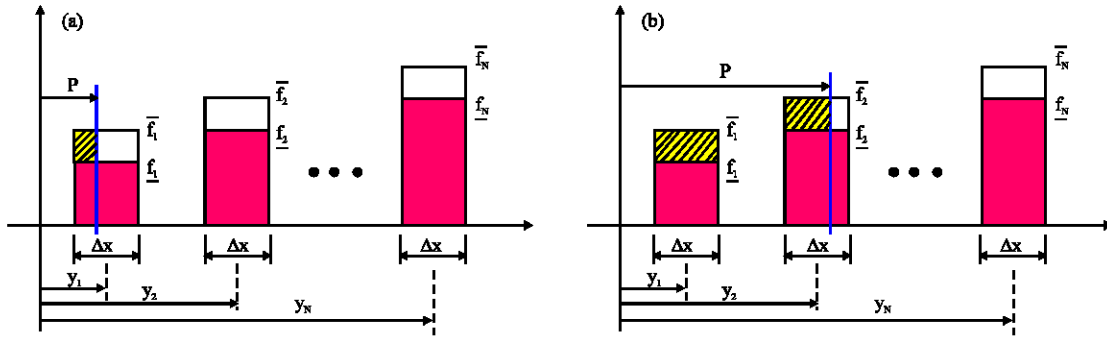


Fig. 7: Graphic illustration of computing the left-most point of the interval output set with the COS method. (a) Determination of the implication at the first singleton and (b) Determination of the implication at the second singleton

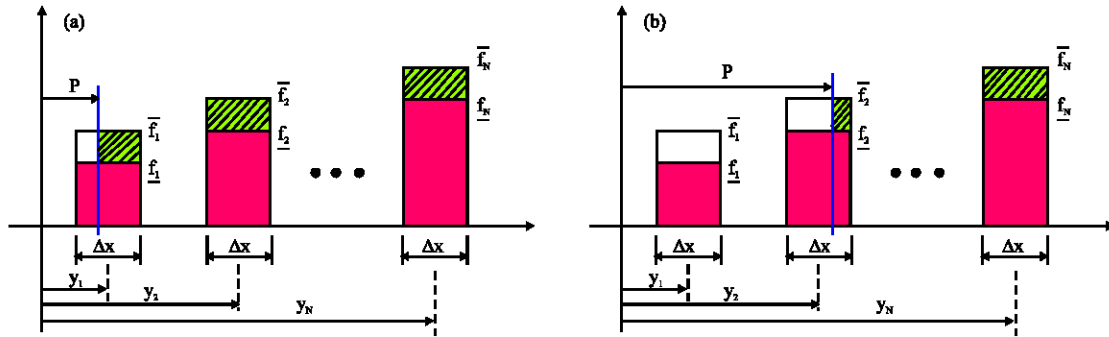


Fig. 8: Graphic illustration of computing the right-most point of an interval output set with the COS method. (a) Determination of the implication at the first singleton and (b) Determination of the implication at the second singleton

$$C_R = \frac{\sum_{i=1}^N \Delta x \cdot \bar{f}_i \cdot y_i - (\bar{f}_k - f_k) \left[P - \left(y_k - \frac{\Delta x}{2} \right) \right] \cdot \left[\left(y_k - \frac{\Delta x}{2} \right) + \frac{P - \left(y_k - \frac{\Delta x}{2} \right)}{2} \right]}{\Delta x \left(\sum_{i=1}^N \bar{f}_i \right) - (\bar{f}_k - f_k) \left[P - \left(y_k - \frac{\Delta x}{2} \right) \right]}$$

$$= \frac{\Delta x \left(\sum_{i=1}^N \bar{f}_i \cdot y_i \right) - (\bar{f}_k - f_k) \left[P - \left(y_k - \frac{\Delta x}{2} \right) \right] \cdot \left[\left(\frac{y_k - \frac{\Delta x}{2}}{2} - \frac{\Delta x}{4} + \frac{P}{2} \right) \right]}{\Delta x \left(\sum_{i=1}^N \bar{f}_i \right) - (\bar{f}_k - f_k) \left[P - \left(y_k - \frac{\Delta x}{2} \right) \right]} \quad (19)$$

where, Δx is the span of uncertainty and y_i is the i -th centroid of the consequent output set.

While point P intersects the second or beyond the second output set, shown in Fig. 8b, C_R can also be calculated by using the center of gravity approach.

$$C_R = \frac{\Delta x \left(\sum_{i=1}^N \bar{f}_i \cdot y_i \right) - \Delta x \cdot \sum_{j=1}^{k-1} (\bar{f}_j - f_j) \cdot y_j - (\bar{f}_k - f_k) \left[P - \left(y_k - \frac{\Delta x}{2} \right) \right] \cdot \left[\left(\frac{y_k - \frac{\Delta x}{2}}{2} - \frac{\Delta x}{4} + \frac{P}{2} \right) \right]}{\Delta x \left(\sum_{i=1}^N \bar{f}_i \right) - \Delta x \cdot \sum_{j=1}^{k-1} (\bar{f}_j - f_j) - (\bar{f}_k - f_k) \left[P - \left(y_k - \frac{\Delta x}{2} \right) \right]} \quad (20)$$

where, N is the number of triggered membership functions. The parameter k can be obtained by the following If-Then rule

$$\text{If } P > \left(y_i - \frac{\Delta x}{2} \right) \text{ then } k = i \quad (21)$$

Similarly, the iteration procedures to obtain the minimum value of $C_{R_{max}}$ are described as follows:

- Step 1:** Set $n = n+1$
- Step 2:** Compute $C_R(n)$
- Step 3:** If $(1 < n)$ and $(n \leq M)$, then $C_R(n) = \max[C_R(n-1), C_R(n)]$
- Step 4:** If $n = M$ then stop.
- Step 5:** Return to step 1

Defuzzifier: From the type-reduction stage, we have type-reduced sets determined by their left-most points and right-most points. We defuzzify the interval set by using the average among them, i.e., the defuzzified crisp output value is:

$$f(u(k-1), \Delta u(k-1)) = \frac{C_{L_{min}} + C_{R_{max}}}{2} \quad (22)$$

RESULTS AND DISCUSSION

To examine the feasibility and validity of the proposed controller, we apply the developed IT2IC to a third order discrete system and an inverted pendulum system, respectively. Before performing the simulations, a type-2 fuzzy inference graphic interface is first designed with MATLAB (Fausett, 2007) to monitor the controlled system dynamically. This graphic interface can show all the information in the inference process via dynamic graphic illustration, including input variables, membership functions and inference results. The blocks with shaded color represent the region bounded by its upper and lower bounds of uncertainty for singleton shape output membership function, which are showed in Fig. 6-8.

Example 1: Consider a third order discrete system:

$$x(k+1) = \begin{bmatrix} 0.8371 & -2.6949 & 0 \\ 0.0018 & 0.9972 & 0 \\ 0 & 0.0020 & 1 \end{bmatrix} x(k) + \begin{bmatrix} 0.0018 \\ 0 \\ 0 \end{bmatrix} u(k) \quad (23)$$

In example 1, the sampling time is selected as 0.002 sec. The triangular-type membership functions with uncertain width is adopted for the IT2FIC and the rule tables are ranging form 3×3 for simulations. The rule table of T1FLC and T2FLC is shown in Table 2. The output responses and the control input of the system are shown in Fig. 9a and b, respectively. From the time responses shown in Fig. 9a, one can see that IT2FIC can obtain the smallest maximum overshoot and give the best performance among the controllers at the same given conditions. In order to compare the feasibilities of these four controllers, three commonly used performance indexes; Integral of the Absolute Error (IAE), Integral of Square Error (ISE) and Integral of Time Multiplied by Absolute Error (ITAE) are adopted to evaluate the tracking performance of these controllers. These three Performance Indexes (PIs) are defined as:

$$IAE = \sum_{k=1}^N |e(k)| \quad (24)$$

$$ISE = \sum_{k=1}^N e^2(k) \quad (25)$$

$$ITAE = \sum_{k=1}^N |e(k)| \times kT \quad (26)$$

where, $N = T_f/T$, T_f is the final time of the simulation and T is the sampling time.

Table 2: Rule table for T1FLC and IT2FLC

u(k)	$\Delta e(k)$		
	N	Z	P
e(k)			
N	N	N	Z
Z	N	Z	P
P	Z	P	P

Table 3: Performance comparisons among four controllers in Example 1

Controller	IAE	ISE	ITAE
T1FLC	27.425	20.178	1.068
IT2FLC	26.841	19.929	1.048
T1FIC	25.187	19.337	0.826
IT2FIC	24.713	19.314	0.782

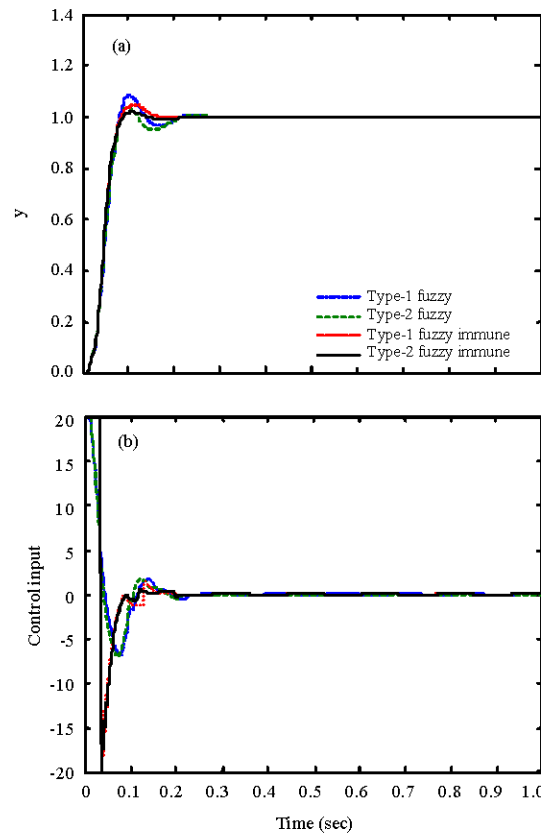


Fig. 9: Time responses of the four closed loop controlled systems. (a) system output (b) control input

The index ITAE is usually utilized to evaluate both transient and steady-state response of the control system. From Table 3, one can find that the IT2FLC gives the best tracking capability among these four controllers and possesses the best performance from these three PIs.

Example 2: An inverted pendulum on a cart, which is also considered by Wang *et al.* (1996), is described as follows.

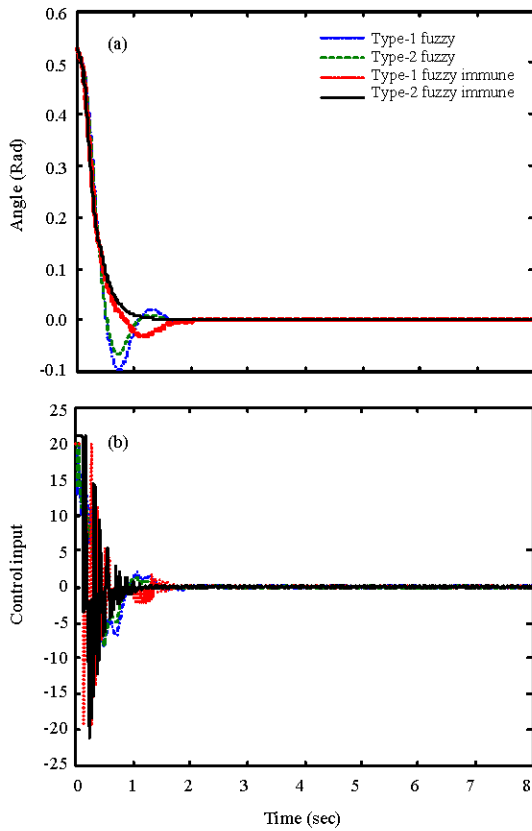


Fig.10: Time responses of the inverted pendulum system. (a) angular displacement (b) control input

Table 4: Performance comparisons among four controllers in Example 2

Controller	IAE	ISE	ITAE
T1FLC	19.802	6.541	6.664
IT2FLC	18.088	6.248	6.121
T1FIC	17.756	5.726	5.642
IT2FIC	17.021	5.661	4.286

$$\begin{aligned} \dot{x}_1 &= x_2 \\ \dot{x}_2 &= \frac{g \sin(x_1) - am\dot{x}_2^2 \sin(2x_1) / 2 - a \cos(x_1)u}{4l/3 - aml \cos^2(x_1)} \end{aligned} \quad (27)$$

where, x_1 is the angle of the pendulum, x_2 is the angular velocity of the pendulum, the mass of the cart is $M = 1$ kg, the mass of the pendulum is $m = 0.05$ kg, $g = 9.8$ m sec⁻² is the acceleration due to gravity, the half length of the pendulum is $l = 1$ m and u is the control input. By using Euler’s method, Eq. 27 can be expressed as:

$$\begin{aligned} x_1(k+1) &= x_1(k) + T x_2(k) \\ x_2(k+1) &= x_2(k) + T \left(\frac{g \sin(x_1(k)) - am\dot{x}_2^2 \sin(2x_1(k)) / 2 - a \cos(x_1)u(k)}{4l/3 - aml \cos^2(x_1(k))} \right) \end{aligned} \quad (28)$$

where, the sampling time T of the pendulum system is 0.01 sec.

In example 2, the triangular-type membership functions with uncertain width and nine rules are exploited for these four controllers; T1FLC, IT2FLC, T1FIC and IT2FIC. Figure 10a shows the simulation results of the proposed methods applied to the inverted pendulum on a cart under the initial condition $x(0) = [\pi/6 \ 0]^T$ and the exogenous disturbance input is $\omega(k) = [0.8e^{-0.04} \cos(k) \ 0.8e^{-0.04} \sin(k)]^T$. All the states can converge to the equilibrium state $[0 \ 0]^T$ after 2 sec as shown in Fig. 10a. The control inputs of the controllers for the system are shown in Fig. 10b.

The indexes of IAE, ISE and ITAE are also exploited to evaluate the tracking performance of these controllers. The performance comparisons of T1FLC, IT2FLC, T1FIC and IT2FIC are shown in Table 4. From Table 4, one can also find that the tracking performance of IT2FLC is the best. From the simulation results and Table 4, one can find that the proposed scheme can provide the best tracking performance than that of other control methods even external disturbance appears.

CONCLUSIONS

In this study, a novel interval type-2 fuzzy immune control has been proposed for linear and nonlinear discrete systems. The IT2FIC combines the immune system and type-2 fuzzy logic control and possesses two features. One is that the IT2FLC can diminish the effect of disturbance than that of T1FLC. The other is that the structure of immune feedback mechanism can make the system output converge to the desired command. A new type-reduction algorithm has been also developed for reducing the computational load. The simulation results demonstrate that the proposed IT2FIC can successfully reduce the disturbance and provide the best tracking performance in comparisons with T1FLC, IT2FLC and T1FIC.

REFERENCES

- Culibrk, D., O. Marques, D. Socek, H. Kalva and B. Furht, 2007. Neural network approach to background modeling for video object segmentation. *IEEE Trans. Neural Networks*, 18: 1614-1627.
- Dianyou, Z., W. Shitong, H. Bin and H. Dewen, 2007. A class of new fuzzy inference systems with linearly parameter growth and without any rule base. *Inform. Technol. J.*, 6: 704-710.
- Fausett, L.V., 2007. *Applied Numerical Analysis Using MATLAB*. Prentice Hall, Upper Saddle River, New Jersey.

- Hsiao, M.Y., C.Y. Chen and T.H.S. Li, 2008. Interval type-2 adaptive fuzzy sliding-mode dynamic control design for wheeled mobile robots. *Int. J. Fuzzy Syst.*, 10: 268-275.
- Hsiao, M.Y., T.H.S. Li, J.Z. Lee, C.H. Chao and S.H. Tsai, 2008. Design of interval type-2 fuzzy sliding-mode controller. *Inform. Sci.*, 178: 1696-1716.
- Kan, J., W. Li and J. Liu, 2008. Fuzzy immune self-tuning PID controller and its simulation. *Proceedings of IEEE International Conference on Industrial Electronics and Applications*, June 3-5, Singapore, pp: 625-628.
- Karnik, N.N. and J.M. Mendel, 1998. Introduction to type-2 fuzzy logic systems. *Proceedings of IEEE FUZZ Conferenc*, May 4-9, Anchorage, AK, pp: 915-920.
- Karnik, N.N., J.M. Mendel and Q. Liang, 1999. Type-2 fuzzy logic systems. *IEEE Trans. Fuzzy Syst.*, 7: 643-658.
- Li, T.H.S., S.H. Tsai, J.Z. Lee, M.Y. Hsiao and C.H. Chao, 2008. Robust fuzzy control for a class of uncertain discrete fuzzy bilinear systems. *IEEE Trans. Syst. Man Cybern. Part B*, 38: 510-527.
- Linfeng, B., C. Fugui and Z. Xiangjin, 2009. Fuzzy adaptive proportional integral and differential with modified smith predictor for micro assembly visual servoing. *Inform. Technol. J.*, 8: 195-201.
- Luh, G.C. and W.W. Liu, 2008. An immunological approach to mobile robot reactive navigation. *Applied Soft Comput.*, 8: 30-45.
- Takahashi, K. and T. Yamada, 1998. Application of an immune feedback mechanism to control systems. *JSME Int. J. Ser. C*, 41: 184-191.
- Visconti, A. and H. Tahayori, 2008. A type-2 fuzzy set recognition algorithm for artificial immune systems. *Lecture Notes Artificial Intel.*, 5271: 491-498.
- Wang, H.O., K. Tanaka and M.F. Griffin, 1996. An approach to fuzzy control of nonlinear systems: Stability and design issues. *IEEE Trans. Fuzzy Syst.*, 4: 14-23.
- Wang, L.X. and J.M. Mendel, 1992. Fuzzy basis functions, universal approximation and OLS. *IEEE Trans. Neural Networks*, 3: 807-814.
- Wu, D. and J.M. Mendel, 2007. Uncertainty measures for interval type-2 fuzzy sets. *Inform. Sci.*, 177: 5378-5393.
- Yu, L., Z. Cai, Z. Jiang and Q. Hu, 2007. An advanced fuzzy immune PID-type tracking controller of a nonholonomic mobile robot. *Proceedings of IEEE International Conference on Automation and Logistics*, Aug. 18-21, Jinan, pp: 66-71.
- Zadeh, L.A., 1975. The concept of a linguistic variable and its application to approximate reasoning. *Inform. Sci.*, 8: 199-249.
- Zhihuan, L., L. Yinhong and D. Xianzhong, 2010. Improved strength pareto evolutionary algorithm with local search strategies for optimal reactive power flow. *Inform. Technol. J.*, 9: 749-757.